

## Research Article

## CFD Simulation and Validation of Interfacial Morphology of Viscous Oil-Water Flow through Upward Inclined Pipe

Anjali Dasari<sup>Å\*</sup>, Bharath Kumar Goshika<sup>Å</sup>, Ravi T. Pilla<sup>Å</sup> and Tapas K. Mandal<sup>Å</sup>

<sup>Å</sup>Department of Chemical Engineering, Indian Institute of Technology, Guwahati – 781039, Assam, India

Accepted 10 January 2014, Available online 01 February 2014, **Special Issue-2, (February 2014)**

### Abstract

Water lubrication technique is one of the most efficient ways to transport viscous oil through pipelines. Flow of two immiscible liquids through conduits gives rise to various flow patterns. In the present study flow patterns of viscous oil-water flow through 5° upward inclined pipeline has been numerically simulated using ANSYS FLUENT™ 6.2. Volume of Fluid (VOF) method has been employed to predict various flow patterns by assuming unsteady flow, immiscible liquid pair (viscous oil and water), constant liquid properties, and co-axial flow. Five flow patterns namely plug flow, slug flow, wavy stratified, stratified mixed and annular flow patterns have been predicted using CFD simulation in upward inclined pipeline. The simulation results have been validated with experimental results. The results gave good proximity with the experimental data.

**Keywords:** Upward inclined, Viscous oil-water, CFD simulation, VOF method, Flow patterns, Prediction.

### 1. Introduction

The simultaneous flow of two immiscible liquids occurs in many chemical and petroleum industries. Nowadays, production and transportation of viscous oil is getting importance due to exhaustion of lighter oil. There are several methods to transport viscous oils, out of these methods water-lubricated transport emerges as an energy efficient technology in the last few decades. During their (oil and water) concurrent flow in a pipe, the deformable interface of the two fluids can attain a variety of characteristic configurations known as flow patterns which strongly depends on fluid properties, pipe inclination and diameter. The flow patterns can be generally grouped into two categories separated and dispersed flows. In separated flows both the phases retain their continuity; one phase flows over the other with complete separation (stratified flow), or there may be inter dispersion of one phase into the other (dual continuous and three layer flow) and at certain conditions lighter phase is enveloped by the heavier one (annular flow). In dispersed flows one phase is continuous and the other one is in the form of dispersed drops. The dispersed phase may occupy a part of the cross section or the entire cross section of the pipe. Small deviation in the inclination of the pipeline has great effect on flow pattern and its transitions. Several researchers carried out experimental and theoretical studies on inclined pipes. The experimental studies have been reported by Mukherjee, *et al.*, 1981, Cox, 1985, Vigneaux, *et al.*, 1988, Hassan and Kabir, 1999, Oddie, *et al.*, 2003,

Xu, *et al.*, 2010, Zong, *et al.*, 2012 on higher inclination pipes and Vedapuri, 1997, Alkaya, 2000, Angeli, *et al.*, 2002, Lum, *et al.*, 2004, Rodriguez and Oliemans, 2006, Grassi, *et al.*, 2008, Kumara, *et al.*, 2010, Castro, *et al.*, 2012 on low inclination pipes.

Besides the experimental works, several authors predicted flow patterns theoretically following analytical approaches (Brauner 2001, Brauner and Ullmann 2002), artificial neural network (ANN) techniques (Sharma *et al.* 2006, Julia *et al.* 2011, Dasari *et al.* 2013) and CFD simulations (Walvekar, *et al.*, 2009, Gosh, *et al.* 2010, Kaushik, *et al.* 2012) in horizontal liquid-liquid flows. Work on CFD simulations for prediction of flow patterns is limited in liquid-liquid flow. Walvekar, *et al.*, 2009, numerically simulated dispersed flow of two immiscible liquids in horizontal pipe line using commercial CFD package in conjunction with multiphase flow model. Gosh, *et al.* 2010 has been predicted the core annular flow pattern in downward flow using k-ε model in volume of fluid (VOF) technique. Al-Yaari and Abu-Sharkh, 2011 simulated the stratified oil-water flow through horizontal pipe using VOF multiphase flow approach coupling with RNG (Re-Normalisation Group) k-ε turbulence model. Later on Kaushik, *et al.* 2012, predicted core annular flow in sudden expansion and contraction in horizontal pipe. They implemented Eulerian-Eulerian based VOF technique for the simulations.

The above literature review shows that numerical simulation of flow patterns for inclined two-phase flow is not available in literature. In the present study an interest was felt to numerically simulate the flow patterns of viscous oil-water flow through 5° upward inclined pipeline

\*Corresponding author: Anjali Dasari

using ANSYS FLUENT™ 6.2. The simulated results have also been validated with the experimental results.

**2. Model development**

The flow domain has been constructed and meshed in GAMBIT™ and the solver chosen is ANSYS FLUENT™. The geometry consists of a 5° upward inclined pipeline with internal diameter of 0.025 m and material of construction used for the pipe is Perspex. The dimensions of the geometry have been shown in Fig. 1. Oil and water were introduced into the pipe through a T- junction at the entry section where water and oil enter into the pipe from the horizontal and vertical directions, respectively. The geometry of the system can be assumed to consist of four sections-water inlet, oil inlet, outlet of the pipe and the test section. An immiscible pair of liquids is chosen with coaxial flow assumed. An unsteady state solver has been employed for the computation purpose. Further, the simulations are run in 2-Dimensional geometry. Lubricating oil and water have been used as test fluids the physical properties of the fluids are given in Table 1.

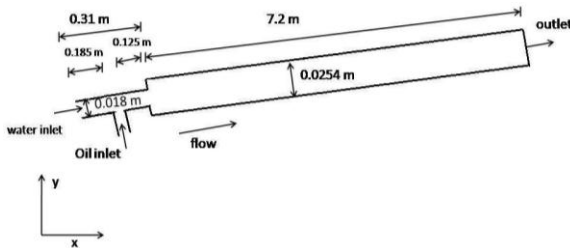


**Fig. 1** Schematic of flow domain and dimension

**Table 1** Physical properties of test fluids

Fluid	Density kg/m <sup>3</sup>	Viscosity Pa s
Water	1000	0.001
Lubricating oil	889	0.107
Interfacial tension	24×10 <sup>-3</sup> N/m	

**2.1 Governing equations**

Modeling of multiphase flow needs special attention due to the presence of number of phases, time, space variant interfaces, multiple scales and large number of interacting phenomena. Considering the hydrodynamics of liquid-liquid flow VOF technique for two-phase flow modeling available in FLUENT has been selected for this case. VOF method solves a single set of momentum equations for both the phases. The details of the governing equations can be obtained from the FLUENT user’s guide (Fluent 6.3 User’s Guide, 2006).

Continuity:

$$\frac{\partial(\rho)}{\partial t} + \nabla \cdot (\rho U) = \sum_q S_q \tag{1}$$

Where,  $\rho$ ,  $U$ ,  $t$ ,  $S$  and  $q$  are density, velocity, time and mass source of  $q^{th}$  phase respectively. In the present case the source term,  $S$  is zero.

Momentum: A single momentum equation is solved throughout the domain and the resulting velocity field is shared among the phases. It can be written as

$$\frac{\partial(\rho U)}{\partial t} + \nabla \cdot (\rho U U) = -\nabla P + \nabla \cdot [\mu(\nabla U + \nabla U^T)] + (\rho g) + F \tag{2}$$

Where  $P$ ,  $g$ ,  $F$ ,  $\mu$  are pressure in the flow field, acceleration due to gravity, body force acting on the system and viscosity of the flowing fluid, respectively.

**2.2 Secondary phase tracking**

The VOF method calculates the volume fraction of each liquid in each cell throughout the domain. In each control volume, the fraction of all the phases sum up to unity. In this method all variables and physical properties are shared by each fluid. Since volume fraction of each phase is known at each location the physical properties of phases are represented by volume averaged values. From these properties we can trace the presence of either of phases or mixture of them depending upon the volume fraction values. In another way, if the volume fraction of  $q^{th}$  in the cell is denoted as  $\alpha_q$ , then the probable situations are

- $\alpha_q = 0$ : the cell does not contain any fluid  $q$ .
- $\alpha_q = 1$ : the cell is occupied solely by fluid  $q$ .
- $0 < \alpha_q < 1$ : the cell contains the interface

Based on the local volume fraction in each cell the appropriate variables and properties are calculated in each control volume within the computational domain. The density and viscosity are estimated as

$$\rho = \sum_1^p \rho_q \alpha_q \tag{3}$$

$$\mu = \sum_1^p \mu_q \alpha_q \tag{4}$$

A separate continuity equation for  $\alpha_q$  is considered as follows

$$\frac{\partial \alpha_q}{\partial t} + (U_q \cdot \Delta) = S_{\alpha_q} \tag{5}$$

For each cell the following relation is also valid

$$\sum_1^p \alpha_q = 1 \tag{6}$$

Here  $p$  is the number of phases, in case of two-phase flow  $p = 2$ .

**2.3. Interface treatment**

VOF model makes use of a piecewise-linear approach to construct interface between two fluids. It assumes that the interface between the two fluids has linear slop within each cell. Based on the information about the volume fraction and it derivatives in the cell it calculates the position of linear interface relative to the center of each partially filled cell is calculated as a first step of interface reconstruction. After that the advection amount of fluid though each face is calculated using the computed linear interface representation, and information on the normal and tangential velocity distribution on the face. By

balancing the fluxes in the previous step the volume fraction of each cell is attained.

#### 2.4 Surface tension and wall adhesion

The VOF model accounts the surface tension along the interface between the phases. The surface tension model uses the continuum surface force (CSF) model (Brackbill, et al, 1992). In this model surface tension effect is added in the momentum equation with the pressure drop, where the pressure drop is calculated from the surface tension coefficient  $\sigma$  and the surface curvature (through radii  $R_1$  and  $R_2$ ) by the Young Laplace equation as follows:

$$\Delta P = \sigma \left( \frac{1}{R_1} + \frac{1}{R_2} \right) \quad (7)$$

$\Delta P$  is the pressure drop of two fluids on either side of the interface.

#### 2.5. Initial and boundary condition

In all the cases the flow has been initialized by filling the pipe with water from the water inlet at a particular superficial velocity and then oil has been introduced into the pipe.

##### 2.5.1. Inlet boundary conditions

The oil velocity is specified at the oil inlet and water velocity at water inlet in the entry section. Thus considering the uniform velocity distribution the velocity conditions are:

- At  $x=0, y=0$ ;  $U_x = U_{\text{water}}$  and  $U_y = 0$
- At  $x = 0.185 \text{ m}$  and  $y = -0.08 \text{ m}$ ,  $U_y = U_{\text{oil}}$  and  $U_x = 0$

##### 2.5.2. Wall boundary conditions

A stationary no slip, no penetration boundary condition is imposed on the pipe wall. In addition the contact angle has been provided during the simulation is  $8.45^\circ$  to account the wall wetting behavior of the fluids with pipe wall.

##### 2.5.3. Outlet boundary conditions

At the outlet of the pipe pressure outlet condition has been selected and the diffusion flux for the variables are set at zero.

### 3. Numerical simulation

#### 3.1. Meshing of the model

The meshing of the 2D geometry has been done using GAMBIT software. Fig.2 shows the meshed geometry of the pipeline. The mesh consists of 2707 and 44248 quadrilateral mesh elements on the entry section and the pipe line respectively. Quadrilateral meshing scheme has been selected to account the surface tension effect more precisely. In order to capture the hydrodynamics at the interface the numbers of grids are higher at the interface

than the film area. To check the dependence of the results on the density of the mesh, a grid independence study has been conducted. It has been identified that the present model is independent of density of the mesh.

Fig. 2 Meshed form of flow domain

#### 3.1. Discretization methods

Two-phase flow is dynamic in nature due to this variation of flow phenomena both in time and space has been considered in the simulations. A transient simulation has been conducted with a time step of 0.001 s. continuity equation has been discretized by PRESTO algorithm (Patankar, 1980) while the momentum equations are discretized by first order upwind method. For pressure velocity coupling PISO (Issa, 1986) algorithm has been used.

#### 3.2. Solution Methodology

Both the phases are introduced at their respective inlets and the transient simulation has been started. The superficial velocities of both oil and water are corresponding to the given experimental conditions have been set as inlet conditions. Then all the above mentioned equations are solved in Fluent by VOF method. The equations are first converted into algebraic forms which are then solved numerically. Unsteady state and pressure based solver were employed in this case. The time step used in the following computations is 0.001s. The equations are integrated over the control volume and the parameters (pressure and velocity) are conserved by solving the momentum and continuity equations using the PISO pressure-velocity coupling scheme. The continuity equations have been discretized using PRESTO algorithm while the momentum equations make use of a first order upwind discretization scheme. For the interface, VOF uses the Geometric Reconstruct interpolation scheme. After few time steps, the flow of both the phases has been identified to track the formation of flow patterns.

### 4. Experimentation

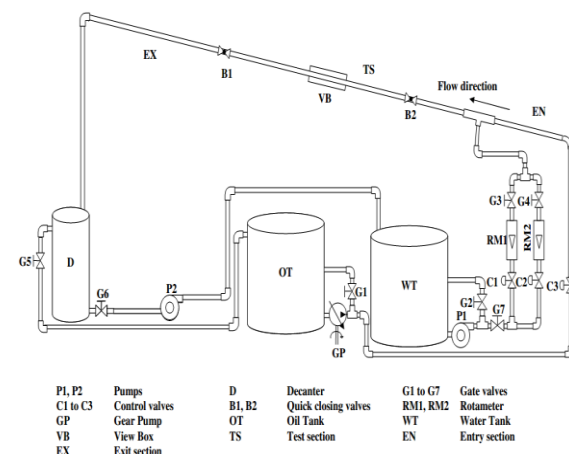


Fig. 3 Schematic representation of experimental setup

In order to validate the simulation results experiments have been conducted in 5° upward inclined pipeline with lubricating oil ( $\rho = 889 \text{ kg/m}^3$ ,  $\mu = 0.107 \text{ Pa s}$ ) and filtered water ( $\rho = 1000 \text{ kg/m}^3$ ,  $\mu = 0.001 \text{ Pa s}$ ) as test fluids. The schematic representation of experimental setup has been shown in Fig. 3. It consists of an entry section (EN), a test section (TS) and an exit (EX) section in the direction of the flow. Test section is made up of 0.025 m internal diameter PMMA of 1 m length. Transparent pipe material has been selected for visualization and photographic studies.

Oil and water have been circulated into the test section through gear (GP) and centrifugal (CP) pumps respectively. During the experiment water is pumped into the test section first and then oil. After reaching the steady state, observations have been noted for the flow phenomena and snap shots are taken by a camera (Model no: DSC-HX100V, Make: Sony) at the view box in test section. Flow patterns have been identified by analyzing these images. Reproducibility of the flow patterns has also been checked and in all the flow patterns more than 99% of reproducibility has been observed. Next set of experiments are conducted by increasing the oil superficial velocity to the next higher value by keeping water superficial velocity constant. Experiments have been performed for a wide range of superficial velocities ( $U_{SO} = 0.052$  to  $1.38 \text{ m/s}$  and  $U_{SW} = 0.068$  to  $1.23 \text{ m/s}$ ) of both the liquids to get all the probable flow patterns.

## 5. Results and discussion

### 5.1. Experimental results

Seven different flow patterns have been observed in the present experimental range such as plug (P), slug (S), wavy stratified (SW), stratified mixed (SM), Annular (A), oil dispersed in water ( $D_{O/W}$ ) and water dispersed in oil ( $D_{W/O}$ ) flow patterns. The photographs of the flow patterns observed in the experimental study have been given in Fig. 4. At lower superficial velocities of both the fluids small oil plugs have been swarming periodically in the continuous water medium, such type of flow pattern is known as plug flow as shown in Fig. 4a. The range of this flow pattern is varied from  $U_{SO} = 0.0045$ - $0.12 \text{ m/s}$  and  $U_{SW} = 0.067$ - $0.567 \text{ m/s}$ .



a. Plug flow ( $U_{SO} = 0.043 \text{ m/s}$  and  $U_{SW} = 0.17 \text{ m/s}$ )



b. Slug flow ( $U_{SO} = 0.095 \text{ m/s}$  and  $U_{SW} = 0.136 \text{ m/s}$ )



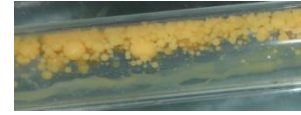
c. Wavy stratified flow ( $U_{SO} = 0.07 \text{ m/s}$  and  $U_{SW} = 0.17 \text{ m/s}$ )



d. Stratified mixed flow ( $U_{SO} = 0.3 \text{ m/s}$  and  $U_{SW} = 0.237 \text{ m/s}$ )



e. Annular flow ( $U_{SO} = 0.3 \text{ m/s}$  and  $U_{SW} = 0.237 \text{ m/s}$ )



f. Dispersion of oil in water flow ( $U_{SO} = 0.176 \text{ m/s}$  and  $U_{SW} = 0.48 \text{ m/s}$ )



g. Dispersion of water in oil flow ( $U_{SO} = 0.99 \text{ m/s}$  and  $U_{SW} = 0.33 \text{ m/s}$ )

Fig. 4 Photographs of observed flow patterns

Further increasing the oil superficial velocity the length of the oil plugs increases and the distance between two consecutive oil plugs diminishes resulting slug flow pattern. The photograph of this pattern is given in Fig. 4b. In the present experimental study this pattern exists from  $U_{SO} = 0.008$ - $0.30 \text{ m/s}$  and  $U_{SW} = 0.067$ - $0.567 \text{ m/s}$ . As shown in Fig. 4c stratification of both the phases have been identified with rise in oil superficial velocity resulting wavy stratified flow pattern with waviness at the interface. The waviness at the interface increases with increase in oil superficial velocity and the flow pattern observed within the range of superficial velocities of both the fluids  $U_{SO} = 0.023$ - $0.226 \text{ m/s}$  and  $U_{SW} = 0.067$ - $0.204 \text{ m/s}$ . With further increase in the oil velocity the wavy interface is broken into droplets with stratification of the phases this kind of flow regime is known as stratified mixed flow pattern as shown in Fig. 4d. The map shows that stratified mixed flow pattern has been occupied wide range of superficial velocities of both water and oil phase ( $U_{SW} = 0.067$ - $0.44 \text{ m/s}$  to  $U_{SO} = 0.15$ - $0.63 \text{ m/s}$ ). At moderately higher velocities of oil and water phase a small water layer has been observed on the top of oil layer and the interface is slightly disturbed resulting annular flow (Fig. 4e). The range of annular flow pattern in this study is varying from  $U_{SW} = 0.37$ - $0.8 \text{ m/s}$  to  $U_{SO} = 0.35$ - $0.7 \text{ m/s}$ . at higher flow rates of water and lower flow rates of oil, it is observed that oil droplets are dispersed in the continuous water phase resulting dispersion of oil in water flow pattern (Fig. 4f). It has been investigated at superficial velocities of water and oil is as follows  $U_{SW} = 0.61$ - $1.22 \text{ m/s}$  to  $U_{SO} = 0.134$ - $0.57 \text{ m/s}$ .

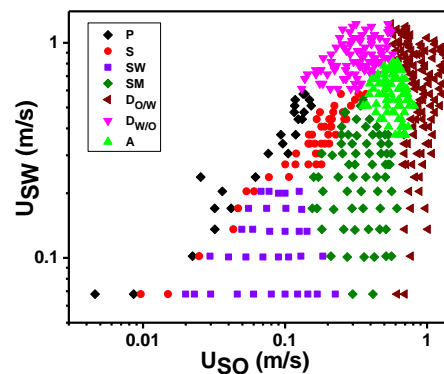
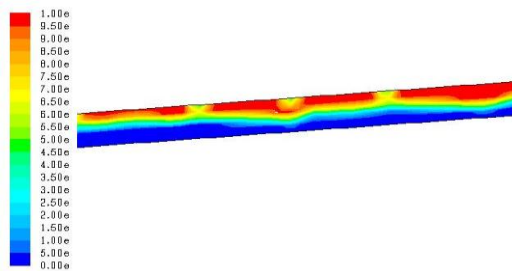


Fig. 5 Experimental flow pattern map

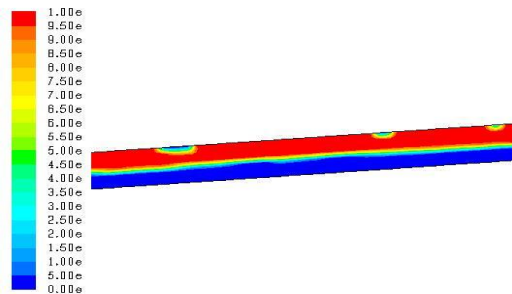
In the same manner at higher flow rates of oil and lower water flow rates, water is completely dispersed in the continuous oil phase this kind of flow phenomena is known as dispersion of water in oil flow pattern. The snapshot of the same is depicted in Fig. 4g and ranges from  $U_{SW}=0.067-1.22$  m/s to  $U_{SO}= 0.615-1.38$ m/s. All the flow patterns investigated during the experimental study have been represented in graphical form known as flow pattern map in Fig.5.

5.2 Simulation results

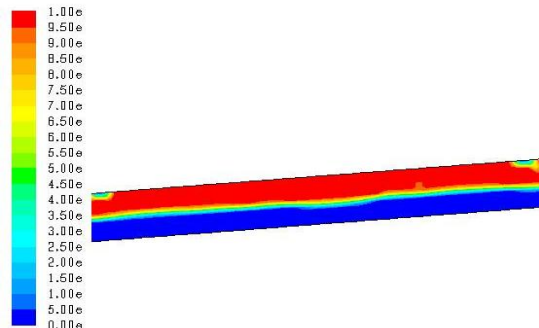
5.2.1. Grid independent study



a) 12,853 Mesh elements



b) 46,955 Mesh elements



c) 61,109 Mesh elements

Fig. 6 Volume fraction contours of oil and water at  $U_{SW} = 0.06$  m/s;  $U_{SO} = 0.14$  m/s

A grid independent study has been conducted with three computational grids of 12,853, 46,955, 61, 109 cells to select the optimum grid size for the computational simulations. Simulations are conducted for one case study

in all the mesh elements mentioned above at  $U_{SW} = 0.06$  m/s;  $U_{SO} = 0.14$  m/s (wavy stratified flow pattern). The volume fraction contours of simulated results for all the mesh elements have been shown in Fig. 6a, b and c respectively.

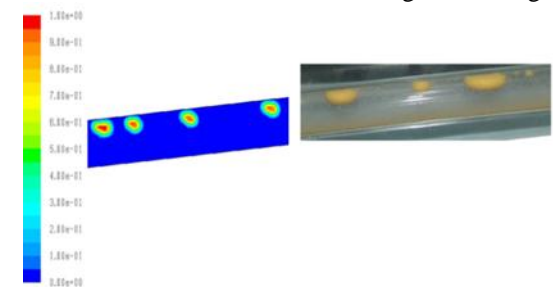
The red colored portion in all the figures represents oil phase and blue portion is water. As shown in Fig. 6a the mesh with 12,853 cells is poor in predicting the wavy stratified flow pattern so extra number of cells is tested at the same flow conditions. Fortunately, systems with 46,955 and 61,109 cells have been given the same volume fraction of oil and water at this flow conditions. Therefore based on the volume fraction contour results 46,955 cells have been selected as optimum number of cells simulation. The mesh consists of 2707 and 44248 quadrilateral mesh elements on the entry section and the pipe line respectively has been selected for the present study.

5.2.1. Prediction of flow patterns

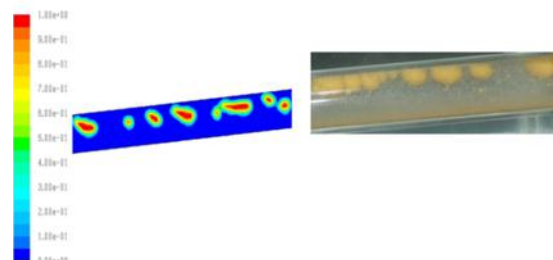
Simulations have been performed by taking various data points in the flow pattern map for five different flow patterns namely plug, slug, wavy stratified, stratified mixed and annular flow.

a. Prediction of plug flow

Simulations have been performed to identify plug flow regime in the range of superficial velocities traced from the flow pattern map (Fig. 5). The results obtained from the CFD simulation and experimental results have been compared here for a pair of superficial velocities of both the fluids. In all the figures volume fraction contours have been shown for the better understanding of the interfacial morphology of oil and water. The blue and red color in the images represents water and oil phases respectively. model, which can be known from the Fig. 7a and Fig. 7b.



a)  $U_{SO} = 0.025$  m/s and  $U_{SW} = 0.27$  m/s



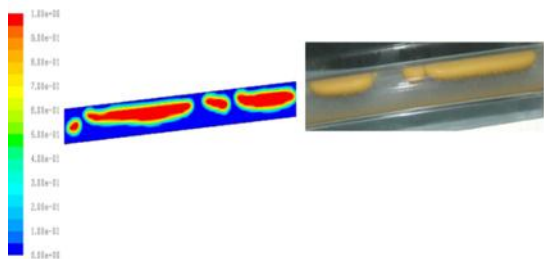
b)  $U_{SO} = 0.1$  m/s and  $U_{SW} = 0.373$  m/s

Fig. 7 Comparison of plug flow results: simulated and experimental

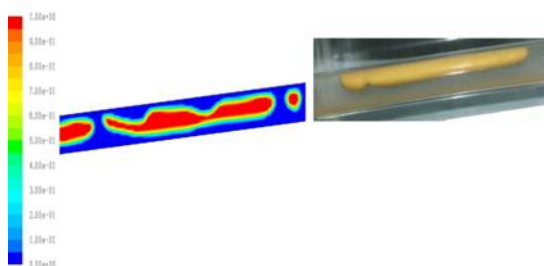
Fig. 7a and Fig. 7b shows the comparison of predicted flow patterns with experimental observations at same flow conditions, which shows good agreement with experimental results. At lower phase superficial velocities the length of liquid bridge between the two consecutive plugs is long, as the velocity increase the length of the liquid bridge decreases and number of oil plugs increases. The size of the oil plugs generally increases with rise in oil velocity such deviation has also been accounted by VOF

*b. Prediction of slug flow*

Simulations have been carried out in the whole range of slug flow identified in the experimental study and the results of two cases are given here. Fig. 8a and Fig. 8b gives the simulated result and photograph slug flow pattern at  $U_{SO}=0.046$  m/s,  $U_{SW} = 0.17$  m/s and  $U_{SO}=0.1$  m/s  $U_{SW} = 0.237$ m/s. The simulated results are in line with the experimental results of the slug flow pattern. From the figures (Fig. 8a and Fig. 8b) it is observed that the length of the oil slug has been increased with enhancement in oil velocity. In the present simulation this effect is clearly shown.



a)  $U_{SO}=0.046$  m/s and  $U_{SW} = 0.17$  m/s



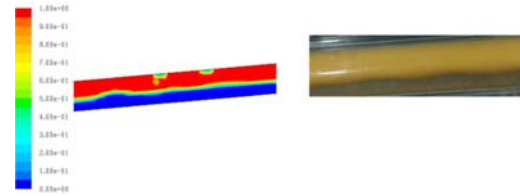
b)  $U_{SO}=0.1$  m/s and  $U_{SW} = 0.237$ m/s

**Fig. 8** Comparison of slug flow results: simulated and experimental

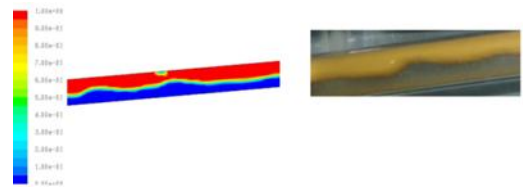
*c. Prediction of wavy stratified flow*

Wavy stratified flow pattern has been predicted from the simulations conducted in the range of superficial velocities of the flow pattern noticed from the experiment and here we are presenting two case studies ( $U_{SO} = 0.13$  m/s,  $U_{SW} = 0.1$  m/s and  $U_{SO} = 0.1$  m/s  $U_{SW} = 0.17$  m/s) for the comparison. The simulated results at these buoyancy conditions have been validated with the experimental results (images of interfacial morphology) at the same flow conditions as shown in Fig. 9a and b. The result

shows that VOF methodology successfully predicted the wavy stratified flow pattern with clear interface with waviness. The amplitude of the waves at the interface increases with enhancement in mixture velocity which is manifestly reflected from the simulated results. This describes that VOF method is capable of predicting this sensitive nature of wave behavior at the interface.



a)  $U_{SO}=0.13$  m/s and  $U_{SW} = 0.1$  m/s

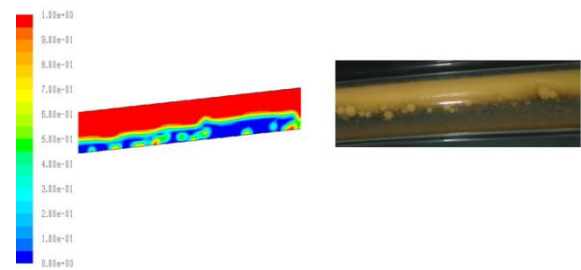


b)  $U_{SO}=0.1$  m/s and  $U_{SW} = 0.17$  m/s

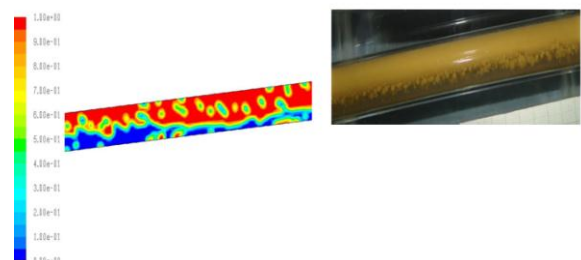
**Fig. 9** Comparison of wavy stratified flow results: simulated and experimental

*d. Prediction of stratified mixed flow*

Stratified mixed flow pattern recognized in the experimental range ( $U_{SW} = 0.067$ - $0.44$ m/s to  $U_{SO}=0.15$ - $0.63$  m/s) has been simulated predict this flow pattern. The simulated results have been compared with the experimental photographs at same flow conditions in Fig. 10a and b.



a)  $U_{SO}=0.37$  m/s and  $U_{SW} = 0.23$  m/s



b)  $U_{SO}=0.468$  m/s and  $U_{SW} = 0.17$  m/s

**Fig. 10** Comparison of stratified mixed flow results: simulated and experimental

The morphology acquired in both the cases is similar to the experimental results. The stratified mixed flow regime has been predicted very well with stratification of phases and oil drops at the interface by VOF method. Fig. 10b reveals that with increase in mixture superficial velocity the number of oil droplets at the interface has been enhanced. This is also properly encountered by VOF technique in predicting stratified mixed flow patten.

e. Prediction of annular flow

Annular flow pattern has been occupied a small region in the experimental flow pattern map. Simulations have been carried out to predict annular flow pattern and the results are depicted in Fig. 11a and b for pair of mixture velocities. Comparison of both experimental and simulation results at same flow conditions shows good prediction of annular flow pattern with VOF technique. Simulations have been carried out at various combinations of superficial velocities to get the entire region of annular flow.

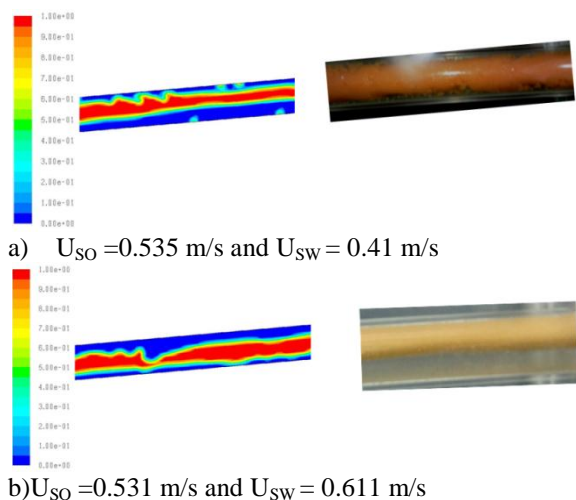


Fig. 11 Comparison of annular flow results: simulated and experimental

6. Validation of simulated results with experiment

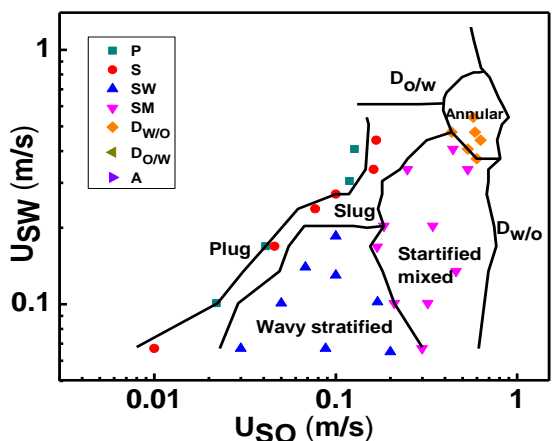


Fig. 12 Simulation results superimposed on experimental flow pattern map

The simulated results are compared with experimental results reported in section 5.1 in order to validate the simulations. For this the simulated points are superimposed on the experimental flow pattern map (Fig. 5) as shown in Fig. 12. The flow pattern map has been represented in terms of  $U_{SO}$  and  $U_{SW}$ . In the figure the curves represents the transition boundaries of flow patterns identified in the experiment and scattered data points denotes the simulated results. All the simulated results are within the experimental region giving the good prediction of interfacial morphologies.

7. Conclusions

Computational fluid dynamic study has been conducted to predict flow patterns of viscous oil-water flow through 5° upward inclined pipeline. Simulations have been conducted in 46,955 cell mesh which is selected based on the grid independence study. Simulations are performed using VOF methodology for plug, slug and separated flows (wavy stratified, stratified mixed and annular flow). All above mentioned flow patterns have been successfully predicted the using CFD package in Fluent 6.2. Seven different flow patterns (plug, slug, wavy stratified, stratified mixed, annular,  $D_{O/W}$  and  $D_{W/O}$ ) have been identified in the present experimental study by visual and photographic technique. The simulated results have been validated with the experimental results. Validation shows good prediction accuracy of all the above mentioned flow patterns. The present results reveal the capability of VOF to predict almost entire flow pattern map with excellent accuracy except two dispersed regions.

Acknowledgements

We thank the CSIR Extramural Research Division-II, Grant No. 22(0573)/12/EMR-II, Government of India, for the financial aid.

References

A.Dasari, A.B.Desamala, A. K. Dasmahapatra, T. K. Mandal,(2013),Experimental studies and PNN prediction on flow pattern of viscous oil-water flow through a circular horizontal pipe, *Industrial Engineering and Chemistry Research*,52, 7975-7985.

A.L. Cox,(1986),A study of horizontal and downhill two-phase oil-water flow, *M.S. Thesis*, The University of Texas.

A.R. Hasan, C.S. Kabir,(1999), A simplified model for oil/water flow in vertical and deviated wellbores. *SPE in Proceedings and Facilities*, 141,56-62.

B. Alkaya,(2000), Oil - Water Flow Patterns and Pressure Gradients in Slightly Inclined Pipes, *M.S. Thesis*, University of Tulsa, USA.

B. Grassi, D. Strazza,(2008), Experimental validation of theoretical models in two - phase high -viscosity ratio of liquid-liquid flows in horizontal and slightly inclined pipes. *Int. J. Multiphase Flow*,34,950-965.

D. Vedapuri, D. Bessette, W.P. Jepsen,(1997), A segregated flow model to predict water layer thickness in oil-water flows in horizontal and slightly inclined pipelines, *In Proceedings Multiphase'97*, Cannes, France, June 18-20,75-105.

Fluent 6.3 User's Guide (2006), Fluent Inc., Lebanon, USA.

- G. Oddie, H. Shi, L.J. Durlofsky, K. Aziz, B. Pfeffer, J.A. Holmes,(2003),Experimental study of two and three phase flows in large diameter inclined pipes. *International Journal of Multiphase Flow*, 29, 527–558.
- H.K.Mukherjee,J.P.Brill,H.D.Beggs,(1981),Experimental Study of Oil-Water Flow in Inclined Pipes, *Transactions of the ASME*, 103, 56-66.
- H.Sharma, G.Das, A. N. Samanta,(2006), ANN-Based prediction of two-phase gas-liquid flow patterns in a circular conduit, *AIChE J*.52, 3018-3028.
- J. E.Julia, B.Ozar, J.J.Jeong, T.Hibiki, M.Ishii, (2011),Flow regime development analysis in adiabatic upward two-phase flow in a vertical annulus. *International Journal of Heat and Fluid Flow*,32, 164–175.
- J.U. Brackbill, D.B. Kothe, C. Zemach,(1992),A continuum method for modeling surface tension, *J. Comput. Phys*, 100, 335–354.
- J.Y.L.Lum,J.Lovick,P.Angeli,(2004), Low inclination oil-water flow, *Can. J. Chem. Eng*, 82,303-315.
- J.Y.Xu,D.HLi, J. Guo, Y.X. wu,(2010),Investigations of phase inversion and frictional pressure gradients in upward and downward oil-water flows in vertical pipes, *International Journal of Multiphase Flow*, 36, 930–939.
- M. A. Al-Yaari, B. F. Abu-Sharkh,(2011),CFD prediction of stratified oil-water flow in a horizontal pipe, *Asian Transactions on Engineering*, 01, 68–75.
- M. S. De Castro, C. C. Pereira, J. N. dos Santos, O. M. H. Rodriguez,(2012),Geometrical and kinematic properties of interfacial waves in stratified oil–water flow in inclined pipe, *Exp. Ther. FluidSci*, 37,171–178.
- N.Brauner, A.Ullmann,(2002), Modeling of phase inversion phenomenon in the two-phase flows, *International Journal of Multiphase Flow*,28, 1177-1204.
- N.Brauner,(2001), The prediction of flow dispersed boundaries in liquid-liquid and gas-liquid systems, *International Journal of Multiphase Flow*,27, 885-910.
- O.M.H.Rodriguez,R.V.A.Oliemans,(2006),Experimental study on oil–water flow in horizontal and slightly inclined pipes, *Int. J. Multiphase Flow*, 32, 323-343.
- P. Vigneaux, P. Chenois, J.P. Hulin,(1988), Liquid-Liquid Flows in an Inclined Pipe, *AIChE Journal*, 34,781-789.
- P.Angeli,S.Lovick, J.Y.L. Lum,(2002), Investigations on the Three-Layer Pattern during L-L Flows, *40th European Two-Phase Flow Group Meeting*, Stockholm, June 10-13.
- R. G. Walvekar, T. S.Y. Choong, S.A. Hussain, M. Khalid, T.G. Chuah,(2009),Numerical study of dispersed oil-water turbulent flow in horizontal pipe, *Journal of Petroleum Science and Engineering*. 65,123–12824.
- R.I.Issa,(1986), Solution of the implicitly discretized fluid flow equations by operator splitting, *Journal of Computational Physics*, 62, 40-65.
- S. Ghosh, G. Das, P. K. Das,(2010), Simulation of core annular down flow through CFD – A comprehensive study, *Chemical Engineering and Processing*, 49, 1222–1228.
- S. V. Patankar,(1980), Numerical heat transfer and fluid flow, Hemisphere, Washington, D.C.
- V.V.R. Kaushik, S. Ghosh, G. Das. P. K. Das,(2012), CFD simulation of core annular flow through sudden contraction and expansion, *Journal of Petroleum Science and Engineering*, 86-87, 153–164.
- W.A.S. Kumara, B.M. Halvorsen, M.C. Melaaen,(2010),Single-beam gamma densitometry measurements of oil – water flow in horizontal and slightly inclined pipes, *International Journal of Multiphase Flow*, 36, 467–480.